Measurement of spin-correlation parameters A_{LL} and A_{SL} in p-p elastic scattering from 500 to 800 MeV

G. Glass, T. S. Bhatia,* J. C. Hiebert, R. A. Kenefick, S. Nath,* L. C. Northcliffe, and W. B. Tippens†
Texas A&M University, College Station, Texas 77843

D. B. Barlow*
Northwestern University, Evanston, Illinois 60201

J. J. Jarmer and J. E. Simmons
Los Alamos National Laboratory, Los Alamos, New Mexico 87545

R. H. Jeppesen
University of Montana, Missoula, Montana 59812

G. E. Tripard
Washington State University, Pullman, Washington 99164
(Received 20 September 1991)

The spin-correlation observable A_{LL} for p-p elastic scattering has been measured at energies 589, 640, 692, 743, and 793 MeV, over a c.m. angular range between 20° and 100°. The spin observable A_{SL} was also measured in this angular range at energies 640 and 793 MeV. At 488 MeV both the spin observables were measured, but only near the c.m. angle of 90°. The data are compared with the predictions of several phase-shift analyses and previous measurements. The energy dependence of A_{LL} for the c.m. angle of 90° is also presented and shows no anomalous behavior. These data provide better angular coverage over five of the energies, with comparable or better statistical precision, than previous measurements of A_{LL}.

PACS number(s): 13.75.Cs, 21.30.+y, 24.70.+s

I. INTRODUCTION

The nucleon-nucleon sector of hadron interactions has always played a major role in the pursuit of a more fundamental understanding of the strong force, and within this sector elastic proton-proton (p-p) scattering is by far the most studied experimentally. The spin-dependent part of the strong interaction is most easily investigated with protons because of the major advances made in the last 30 years with polarized-proton targets and polarized beams from the intermediate-energy region below 1 up to 20 GeV. Phase-shift solutions rely heavily on knowledge of spin-dependent observables, of which many have been measured [1–20] for p-p elastic scattering between 500 and 800 MeV. Even the spin dependence of the p-p total cross section has been studied extensively in this energy region [21,22]. The analyzing power, or polarization parameter, is known to better than 1% relative over most of the intermediate-energy region [12]. The spin-transfer coefficients D_{ij} have also been measured, but with less precision (~5% relative)[9]. Spin-correlation parameters have been determined [1–8], but only for A_{NN} and A_{LL} is the determination extensive. While A_{SS} has been covered moderately at several energies [2,20], there is still a shortage of data for A_{SL}. At 579 MeV there are sufficient measurements to specify all of the complex amplitudes uniquely [16], and with partial-wave analysis (PWA) techniques these amplitudes are determined over the entire angular range. Several triple-spin parameters have been measured at 730 MeV [14], and these have been especially useful where there has been a shortage of the more conventional observables (one and two spin). Despite the abundance of data between 500 and 800 MeV, however, considerable disagreement still exists between several PWA's [23–27], which is usually symptomatic of either poor or insufficient data. The present results should help to remedy a significant deficiency in the current database in this energy region.

II. EXPERIMENTAL METHOD AND ANALYSIS

The equipment for this measurement was identical to that used for a $pp \rightarrow \pi d$ experiment [28], and data for both the reactions were taken concurrently. Therefore, only mention of the differences between the two experiments will be made here. The spectrometer used to measure the scattered proton momentum was set to be roughly centered at c.m. angles 40°, 50°, 60°, 70°, 80°, and 90°

*Present address: Los Alamos National Laboratory, Los Alamos, NM 87545.
†Present address: University of California, Los Angeles, CA 90024.

for nominal beam energies 600, 700, and 800 MeV. A 55° setting was used in lieu of 50° and 60° for 650 MeV, while only 80° and 90° settings were used for 500 MeV. The 50° and 70° settings were also missing from the 750 MeV data. An additional 30° setting was used for 700 and 800 MeV. The proton scattered into the larger angle was detected for all angle settings with at least a scintillator signal in coincidence with the spectrometer. At the 90° c.m. setting both protons were detected in multiwire proportional chambers (MWPC's), on one side with a magnetic spectrometer, and on the other with just MWPC's and scintillators. At the other angle settings, the coils of the polarized target magnet (PTM) obstructed the path of the larger-angle (recoil) proton, and only a small scintillator could be used to detect this proton before it struck the coils. Other than the different kinematic settings required for the case of elastic p-p scattering, all other aspects of this experiment are the same as those described in the $pp \rightarrow \pi d$ paper [28].

Measured time-of-flight spectra and momentum in the spectrometer were used to calculate the detected particle mass and identify protons. When particles were seen in both sets of MWPC's, measurements of the coplanarity and the opening angle of the proton trajectories could be used to extract the elastic-scattering signal. In the more usual case, when no track information was available for the recoil proton, the signal for elastic scattering was determined from the area under a peak in a missing-mass histogram. Missing mass was calculated in terms of the momentum and angle of the protons detected in the spectrometer. At angle settings where two-particle tracking could be used, backgrounds were ~5%, while at the settings where only single-particle tracking was possible, the backgrounds varied between 10% and 30%, a clear demonstration of the well-known benefits of two-particle tracking.

Signal event yields were obtained for each of the four spin configurations corresponding to the beam and target polarization states, (++), (+−), (−+), and (−−), where the signs indicate the sense of polarization for beam and target (beamtarget). Appropriate beam-normalization and live-time factors were applied to the yields, from which backgrounds had been subtracted by the application of fits to the signal histograms. These fits were made up of an asymmetric Gaussian (the signal) and a second-order polynomial (the background). Background data, taken with carbon in place of the polarized target material, were used to verify that these polynomial fits to the background were adequate.

The beam polarization was either pure longitudinal (L) for energies 600, 700, and 750 MeV or a mix of sidewise (S) and longitudinal for 500, 650, and 800 MeV. For the latter three energies two mixtures, usually 90° apart in spin orientation, were used, which enabled a separation of the two spin observables A_{LL} and A_{SL}. For a target with pure L polarization, the cross section can be written in terms of the nonvanishing (parity conserving) spin parameters as

$$\sigma = \sigma_{00}(1 + P_n^b A_{NO} + P_s^b P_l^t A_{SL} + P_l^b P_l^t A_{LL}) , \quad (1)$$

where σ_{00} is the spin-averaged (unpolarized) cross section, P_n^b is the component of beam polarization normal to the scattering plane, P_s^b is the component of transverse beam polarization in the scattering plane (S component), and $P_l^{b(t)}$ is the beam (target) component in the beam direction (L component). The normal component P_n^b results from precession of the original S component of the beam as the incident protons pass through the magnetic field of the polarized target magnet. The scattered protons are also deflected by the magnetic field of the polarized target magnet, and the true scattering plane is determined with an appropriate rotation of the measured scattering plane. Asymmetries ϵ are determined by the expression

$$\epsilon = \frac{(++)+(--)-(+-)-(-+)}{(++)+(--)+(+-)+(-+)} , \quad (2)$$

where ( ) represents the normalized yields in each of the polarization states. Thus the effect of the normal component only shows up to the extent that the (+) and (−) magnitudes for the beam polarization are different. This difference was examined and determined to be small; the worst case would have changed the value of the observables by less than 0.02, which is the order of the statistical error. Therefore, this normal polarization term was left out of the computation of A_{SL} and A_{LL}. Similarly, it was determined that the effect of small differences in magnitude of target polarization in the (+) and (−) states was negligible.

When the beam polarization is purely L, the asymmetry associated with the yields is $\epsilon_L = P_l^b P_l^t A_{LL}$. When the beam contains both L and S components of polarization, two different mixtures of beam polarization are used, differing usually by a 90° precession. Thus two different asymmetries ϵ_1 and ϵ_2 are measured, where $\epsilon_i = P_{il}^t (P_{is}^b A_{SL} + P_{il}^b A_{LL})$, where i designates each of the two beam spin orientations at the target. The asymmetries associated with the yields are thus a result of a linear combination of A_{SL} and A_{LL}, and Eq. (2) is used for each value of i to get two independent linear equations for A_{SL} and A_{LL}, the solution being

$$A_{LL} = \frac{a_2\epsilon_1 - a_1\epsilon_2}{D} , \quad A_{SL} = \frac{b_1\epsilon_2 - b_2\epsilon_1}{D} , \quad (3)$$

where $a_i = P_{il}^t P_{is}^b$, $b_i = P_{il}^t P_{il}^b$, and $D = a_2 b_1 - a_1 b_2$.

Data were taken over the course of several runs with duplication of beam and target polarization states, thus providing the opportunity to check for internal consistency from the value of χ^2. The value of χ^2 is given by the weighted sum of the squares of the difference from the average observable value of all the sets having duplicate settings. When the value of $\chi^2/(n-1)$ was ≥ 2 for n sets of data, the statistical error was increased by a factor $\sqrt{\chi^2/(n-1)}$. Each angle setting was divided into five bins, each of which covered an angular width of ~2° c.m.

III. RESULTS AND DISCUSSION

In Table I the beam energy at the center of the polarized target is given for each of the nominal (initial) beam energies. The difference is due to energy loss of the beam

TABLE I. Beam energy at the target center after energy-loss corrections.

Initial energy (MeV)	At target center (MeV)
500	488
600	589
650	640
700	692
750	743
800	793

in material upstream of the target center [28]. The values for the measured observables A_{LL} and A_{SL} are given in Tables II and III. In Figs. 1 through 6 the observable A_{LL} is plotted along with various phase-shift analysis (PSA) predictions. Note that the present data have not been included in any of the databases for the various PSA's. Also shown in these plots are data from some previous experiments. The agreement is generally good except for overall normalization, although there is some discrepancy, even in the angular distribution, between the present results and those of Auer *et al.* [4] between 740

TABLE II. The A_{LL} results.

$\Theta_{c.m.}$	A_{LL}	ΔA_{LL}	$\Theta_{c.m.}$	A_{LL}	ΔA_{LL}	$\Theta_{c.m.}$	A_{LL}	ΔA_{LL}	$\Theta_{c.m.}$	A_{LL}	ΔA_{LL}
		$T_0=488$ MeV				37.5	0.318	0.010	72.4	0.256	0.017
72.7	0.243	0.070	85.7	0.128	0.022	39.9	0.305	0.019	74.5	0.199	0.021
75.4	0.159	0.023	87.5	0.151	0.016	43.0	0.266	0.009	75.9	0.164	0.037
77.9	0.077	0.027	89.9	0.157	0.017	45.4	0.228	0.014	78.2	0.201	0.031
81.3	0.146	0.123	92.3	0.139	0.021	45.7	0.206	0.012	80.5	0.216	0.027
94.5	0.143	0.026				48.0	0.246	0.012	83.0	0.245	0.024
						50.4	0.226	0.013	85.4	0.234	0.023
		$T_0=589$ MeV				53.0	0.233	0.012	85.8	0.232	0.033
35.5	0.390	0.015	65.2	0.290	0.020	54.7	0.234	0.016	87.5	0.271	0.043
37.5	0.365	0.019	66.0	0.276	0.016	55.4	0.207	0.021	90.0	0.219	0.021
39.9	0.356	0.011	69.0	0.245	0.041	57.2	0.248	0.016	92.4	0.268	0.019
43.0	0.360	0.011	71.4	0.219	0.017	60.7	0.219	0.015	94.5	0.234	0.023
45.5	0.310	0.015	73.4	0.211	0.023	63.4	0.248	0.016			
45.5	0.309	0.026	75.7	0.187	0.024						
48.0	0.291	0.030	78.2	0.162	0.025						
50.4	0.325	0.015	80.5	0.173	0.025			$T_0=743$ MeV			
53.0	0.298	0.030	83.0	0.185	0.016	36.6	0.301	0.016	75.9	0.209	0.033
55.4	0.309	0.049	85.2	0.165	0.027	38.5	0.239	0.012	78.2	0.224	0.022
55.6	0.296	0.027	85.8	0.191	0.025	40.9	0.230	0.012	80.5	0.261	0.027
58.0	0.301	0.013	87.5	0.177	0.021	43.9	0.205	0.011	82.5	0.250	0.048
60.5	0.279	0.014	89.9	0.200	0.019	46.4	0.223	0.027	84.4	0.245	0.020
62.9	0.250	0.013	92.4	0.187	0.026	55.6	0.187	0.015	85.8	0.214	0.046
63.8	0.267	0.021	94.5	0.143	0.035	58.0	0.196	0.029	87.5	0.216	0.033
						60.9	0.208	0.013	90.0	0.244	0.018
		$T_0=640$ MeV				63.4	0.216	0.014	92.4	0.221	0.017
34.9	0.331	0.040	72.4	0.237	0.015	65.4	0.205	0.023	94.5	0.181	0.020
37.2	0.316	0.032	74.6	0.193	0.017						
39.4	0.310	0.015	74.9	0.270	0.058						
42.0	0.307	0.027	77.0	0.231	0.017			$T_0=793$ MeV			
44.9	0.289	0.017	79.4	0.197	0.018	29.6	0.371	0.017	65.6	0.197	0.019
50.2	0.235	0.016	81.4	0.216	0.019	31.5	0.362	0.023	67.5	0.182	0.017
52.0	0.263	0.011	83.7	0.238	0.022	33.3	0.322	0.015	69.9	0.206	0.015
54.9	0.254	0.011	85.8	0.158	0.056	36.9	0.285	0.015	72.4	0.216	0.018
57.9	0.233	0.011	87.5	0.272	0.032	38.5	0.276	0.010	74.6	0.210	0.019
60.2	0.223	0.015	89.9	0.151	0.052	40.9	0.250	0.023	75.8	0.170	0.031
65.6	0.278	0.037	92.4	0.189	0.038	44.0	0.247	0.017	78.2	0.214	0.023
67.5	0.221	0.029	94.5	0.214	0.030	46.2	0.210	0.018	80.5	0.224	0.021
69.9	0.257	0.015				48.0	0.226	0.011	82.5	0.215	0.020
						50.4	0.200	0.011	84.4	0.232	0.021
		$T_0=692$ MeV				52.9	0.205	0.025	85.8	0.215	0.035
28.6	0.331	0.017	65.6	0.279	0.021	55.7	0.194	0.016	87.5	0.231	0.021
31.1	0.343	0.011	65.7	0.276	0.029	55.7	0.194	0.016	90.0	0.193	0.020
33.5	0.312	0.010	67.5	0.236	0.017	57.9	0.203	0.022	92.4	0.258	0.019
35.7	0.308	0.028	69.9	0.202	0.026	60.9	0.185	0.024	94.5	0.223	0.023
						63.4	0.186	0.024			

TABLE III. The A_{SL} results.

$\Theta_{c.m.}$	A_{SL}	ΔA_{SL}	$\Theta_{c.m.}$	A_{SL}	ΔA_{SL}
		$T_0=488$ MeV			
72.7	0.071	0.052	87.5	−0.028	0.017
75.4	0.002	0.053	89.9	0.014	0.022
77.9	0.159	0.053	92.3	0.021	0.018
85.7	−0.025	0.021	94.5	0.091	0.023
		$T_0=640$ MeV			
34.9	−0.179	0.021	72.4	−0.017	0.017
37.2	−0.117	0.039	74.6	0.028	0.021
39.4	−0.100	0.015	74.9	−0.013	0.074
42.0	−0.094	0.022	77.0	0.006	0.020
44.9	−0.110	0.015	79.4	−0.015	0.022
50.2	−0.043	0.025	81.4	−0.008	0.043
52.0	−0.073	0.015	83.7	0.042	0.027
54.9	−0.017	0.014	85.8	−0.016	0.096
57.9	−0.049	0.014	87.5	0.021	0.061
60.2	0.000	0.017	89.9	0.009	0.030
65.6	−0.035	0.024	92.4	0.105	0.101
67.5	−0.004	0.026	94.5	−0.026	0.028
69.9	−0.004	0.027			
		$T_0=793$ MeV			
29.6	−0.071	0.027	65.6	0.009	0.035
31.5	−0.028	0.040	65.6	0.065	0.023
33.3	−0.053	0.016	67.5	0.056	0.018
36.9	−0.031	0.016	69.9	0.047	0.017
38.5	−0.035	0.011	72.4	0.050	0.019
40.9	−0.029	0.017	74.6	−0.029	0.021
44.0	0.005	0.013	75.8	0.083	0.036
46.1	−0.047	0.020	78.2	−0.028	0.026
46.4	0.046	0.044	80.5	0.002	0.023
48.0	−0.042	0.011	82.5	0.013	0.022
50.4	−0.015	0.011	84.4	−0.002	0.022
52.9	−0.003	0.018	85.8	−0.055	0.053
55.7	−0.027	0.020	87.5	0.008	0.023
55.7	0.015	0.016	90.0	0.040	0.021
57.9	0.030	0.017	92.4	−0.031	0.030
60.9	0.021	0.014	94.5	−0.014	0.032
63.4	0.008	0.019			

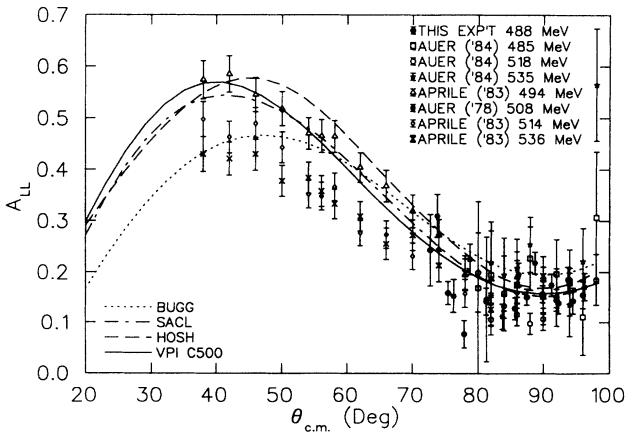

FIG. 1. Present results for A_{LL} at 488 MeV, along with the PSA predictions of Hoshizaki (HOSH) [23], Bystricky (SACL) [24], Arndt *et al.*, (VPI) [25], and Bugg [26]. The measurements of Auer *et al.* [4] at 485, 518, and 535 MeV, Auer *et al.* [1] at 508 MeV are also shown with Aprile *et al.* [3] at 494, 514, and 536 MeV.

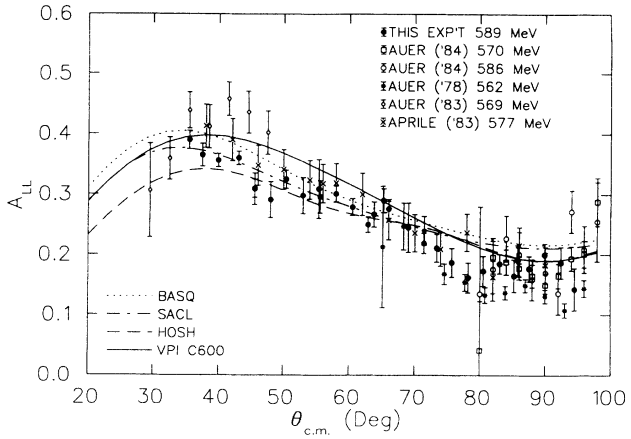

FIG. 2. Present results for A_{LL} at 589 MeV, along with the PSA predictions as identified in Fig. 1, except that here the PSA prediction of Dubois *et al.* (BASQ) [27], replaces BUGG. The previous data are from Auer *et al.* [4] at 570 and 586 MeV, from Auer *et al*, [1] at 562 MeV, and from Auer *et al.* [2] at 569 MeV. The data at 577 MeV are from Aprile *et al.* [3].

and 806 MeV near 90°. There is also some disagreement with the 800 MeV data of Pauletta *et al.* [6], but this could also be just a normalization error. The present results agree remarkably well with the PSA of VPI [25], and almost as well with the Saclay PSA except at 800 MeV. The present results also show lack of agreement with the PSA of Hoshizaki [23] above 500 MeV, which is not surprising in view of the smallness and age of the database associated with that PSA. Although the BASQUE PSA [27] would not be expected to fit very well either, since it has not been updated recently, it fits fairly well at 600, 650, 700, and 750 MeV. At 500 and 800 MeV a recently updated PSA by Bugg [26] is used in place of the BASQUE PSA. The fits are in excellent agreement with the present data, especially at 800 MeV. At 500 MeV, however, Bugg's PSA predictions diverge from those of the other PSA's below 60°. Also at 500 MeV, where all

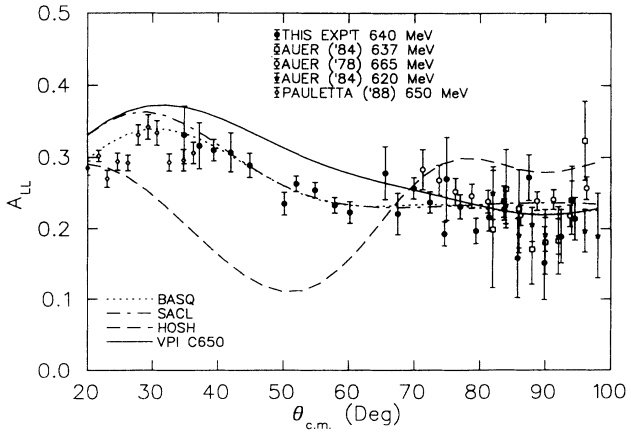

FIG. 3. Present results for A_{LL} at 640 MeV along with the PSA predictions as identified in Fig. 2. The previous data are from Auer *et al.* [4] at 637 and 620 MeV, from Auer *et al.* [1] at 665 MeV, and from Pauletta *et al.* [6] at 650 MeV.

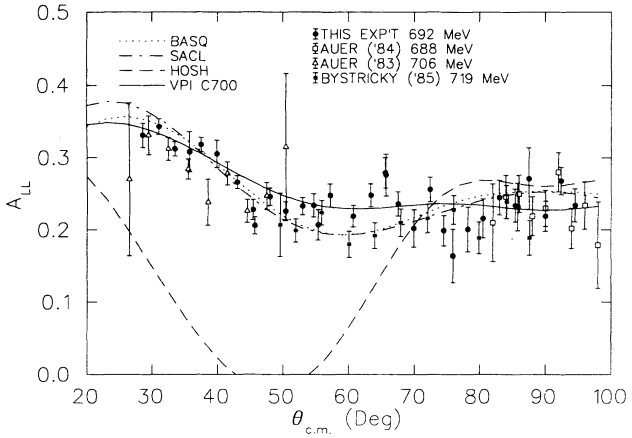

FIG. 4. Present results for A_{LL} at 692 MeV along with the PSA's as identified in Fig. 2. The previous data are from Auer *et al.* [4] at 688 MeV, from Auer *et al.* [2] at 706 MeV, and from Bysricky *et al.* [5] at 719 MeV.

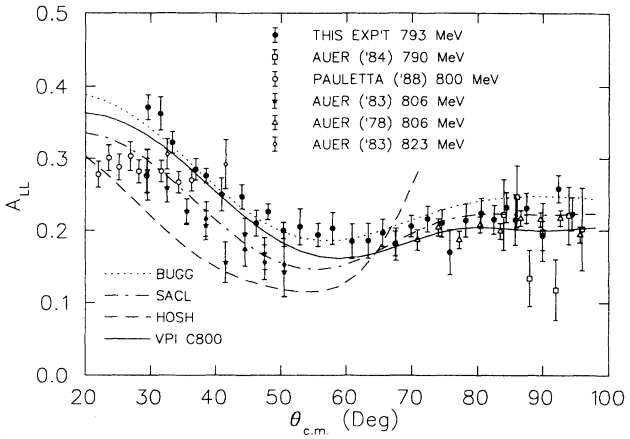

FIG. 6. Present results for A_{LL} at 793 MeV along with the PSA's as identified in Fig. 1. The previous data are from Auer *et al.* [4] at 790 MeV, from Pauletta *et al.* [6] at 800 MeV, from Auer *et al.* [2] at 806 and 823 MeV, and from Auer *et al.* [1] also at 806 MeV.

the PSA fits seem to be in reasonable agreement above 60°, the present data show two points more than three standard deviations from the mean of the PSA fits. Since these data were taken early in the experiment, it is not unreasonable to consider these points as suspect and perhaps should not be included in any of the *p-p* elastic-scattering databases. Note, however, that these points are not too far out of line with the rest of the world's data. At 800 MeV, on the other hand, there is considerable disagreement between the present results and the data of Pauletta *et al.* [6] and Auer *et al.* [1] below 50°, but this again appears to be a normalization discrepancy. The renormalization required the data of Pauletta *et al.* [6] in the VPI PSA [25] is 0.85 whereas the normalization error given by the authors is only ±0.05, which accounts for a very large contribution, ~8, to the χ^2 value for these data.

Plots of the A_{SL} data from this experiment and several others [2–4,7,8] are shown in Figs. 7–9 along with the various PSA predictions. Here again there appears to be good agreement with the VPI [25] and BASQUE [27] or Bugg [26] PSA predictions at 650 and 800 MeV, but not very good agreement with Hoshizaki [23] at these energies. The Saclay [24] PSA prediction is more than a standard deviation from these data over most of the angular range at 800 MeV, which is an indication that the A_{SL} predictions are more sensitive than A_{LL} to the variations in the different PSA's. At 500 MeV three points of the present experiment are significantly out of line with both the PSA's and the rest of the world's data, which may also, as in the A_{LL} measurement, be an indication of problems with the data taken early in the experiment. The systematic error for these early data could be as high as 0.05 due to poor signal determination and large fluc-

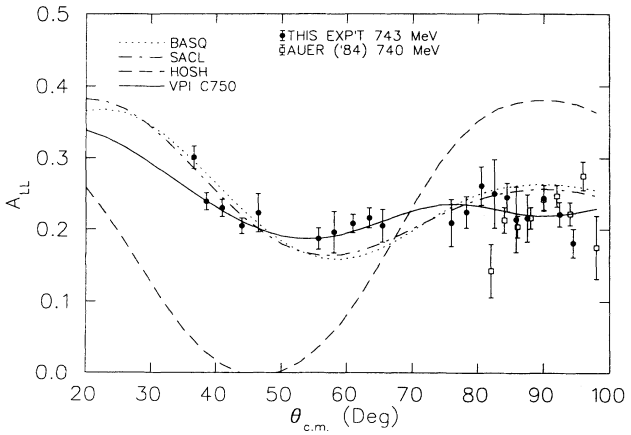

FIG. 5. Present results for A_{LL} at 743 MeV along with the PSA's as identified in Fig. 2. The previous data are from Auer *et al.* [4] at 740 MeV.

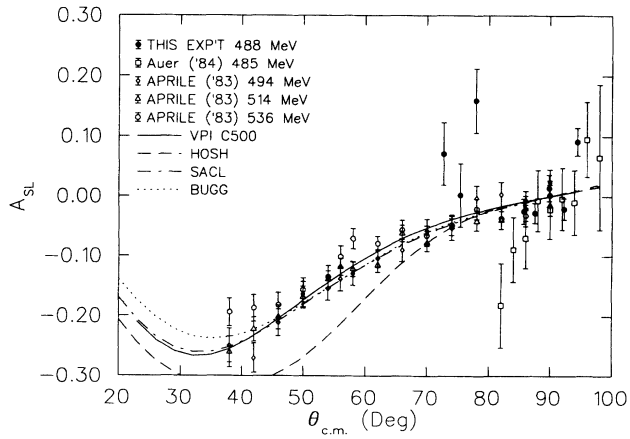

FIG. 7. Present results for A_{SL} at 488 MeV along with the PSA's as identified in Fig. 1. The previous data are from Auer *et al.* [4] at 485 MeV, and from Aprile *et al.* [3] at 494, 514, and 536 MeV.

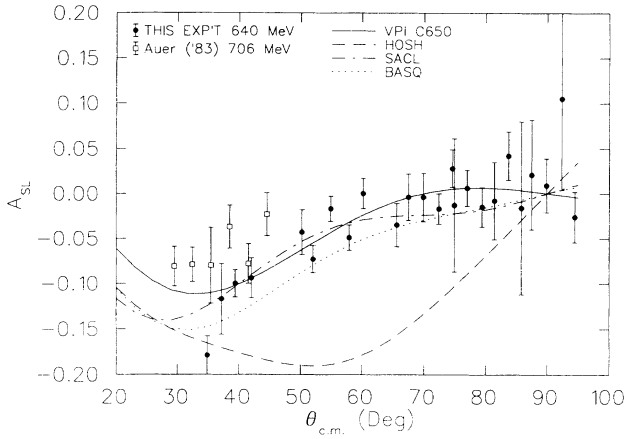

FIG. 8. Present results for A_{SL} at 640 MeV along with the PSA's as identified in Fig. 2. The previous data are from Auer *et al.* [2] at 706 MeV.

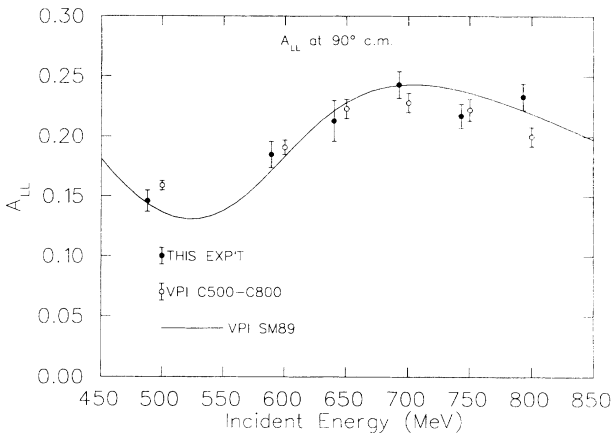

FIG. 10. Values of A_{LL}, averaged over the c.m. angular region 85° to 95°, as a function of incident beam energy, along with the energy-dependent (SM89) and single-energy (C500-C800) PSA solutions of VPI [25].

tuating backgrounds, which could easily vary from point to point, and therefore simulate statistical error. If these 500-MeV data are incorporated into the various databases, their errors should be increased over those shown here by the addition of the systematic error in quadrature. The overall normalization error at each energy is ~4%, while the error due to incorrect background subtractions in the worst cases (excluding the 500-MeV data) are also ~4%—the net systematic error is $\leq \sim 6\%$. This systematic error corresponds to variations from one angle setting to the next, and therefore could be treated as independent from one group of points to the next in each of the angular distributions. The error due to other fluctuations has already been included in the statistical error as stated at the end of Sec. II.

At 90° c.m., special relations connect the observables to some of the amplitudes [29]. Dibaryon or six-quark phenomena may be more evident in the energy dependence of these amplitudes. Therefore, in order to determine whether any anomalies are to be seen in the energy dependence at 90°, the values of A_{LL} averaged over the c.m. angular region 85°–95° are plotted versus the incident energy in Fig. 10. The energy dependence is seen to be smooth and in reasonable agreement with the PSA predictions of VPI [25], except perhaps at 800 MeV, where the results of this experiment differ from the VPI single-energy fit C800 by more than one standard deviation. It is to be noted, however, that the difference between the VPI single-energy solutions C500–C800 and the VPI energy-dependent solution SM89 are comparable to the difference between the experimental points and either fit.

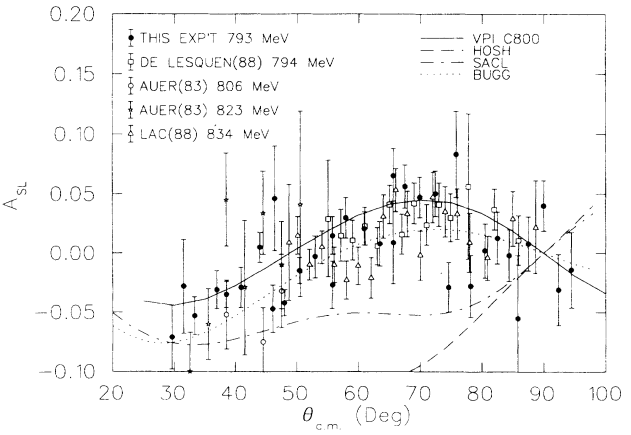

FIG. 9. Present results for A_{SL} at 793 MeV along with the PSA's as identified in Fig. 1. The previous data are from de Lesquen *et al.* [8] at 794 MeV, from Auer *et al.* [2] at 806 and 823 MeV, and from Lac *et al.* [7] at 834 MeV.

IV. CONCLUSIONS

Although there is an abundance of previous data for A_{LL} and A_{SL} in the 500–800 MeV energy region, there is an appreciable spread of values, beyond the statistical uncertainties for the data, implying considerable systematic uncertainty. The overall uncertainty in the final PSA predictions is significantly reduced by the addition of the present measurements. Three of the PSA predictions [25–27], which do not include these data, are in fairly good agreement over the entire energy range covered in this experiment, and have therefore gained considerably in credibility. Thus the $I=1$ phase shifts should be better determined when these data are included in the databases. Finally, although dibaryons have been proposed [23] in the energy range of these measurements, no evidence is seen for them in the energy dependence of A_{LL} at 90° c.m.

ACKNOWLEDGMENTS

The LAMPF staff and management were most helpful in the various phases of this experiment, including the

analysis of the data, which was done at the LAMPF Data Analysis Center. The polarized target also was furnished and maintained by LAMPF personnel. Two of us, RHJ and DBB, would also like to thank the Associated Western Universities for their support. This work was supported in part by the U.S. Department of Energy under Contract No. DE-AS05-76ER04449 and Grant No. DE-FG05-88ER40399.

[1] I. P. Auer *et al.*, Phys. Rev. Lett. **41**, 1436 (1978).
[2] I. P. Auer *et al.*, Phys. Rev. Lett. **51**, 1411 (1983).
[3] E. Aprile, R. Hausammann, E. Heer, R. Hess, C. Lechanoine-Leluc, W. R. Leo, S. Morenzoni, Y. Onel, D. Rapin, and S. Mango, Phys. Rev. D **28**, 21 (1983).
[4] I. P. Auer *et al.*, Phys. Rev. D **29**, 2435 (1984).
[5] J. Bystricky *et al.*, Nucl. Phys. **B258**, 483 (1985).
[6] G. Pauletta *et al.*, Phys. Lett. **211B**, 19 (1988); M. Gazzaly *et al.*, Phys. Rev. Lett. **58**, 1084 (1987).
[7] C. D. Lac *et al.*, Nucl. Phys. **B297**, 653 (1988).
[8] A. de Lesquen *et al.*, Nucl. Phys. **B304**, 673 (1988).
[9] C. L. Hollas *et al.*, Phys. Rev. C **30**, 1251 (1984).
[10] M. W. McNaughton, B. E. Bonner, W. D. Cornelius, E. W. Hoffman, O. B. Van Dyck, R. L. York, R. D. Ransome, C. L. Hollas, P. J. Riley, and K. Toshioka, Phys. Rev. C **25**, 1967 (1982).
[11] M. W. McNaughton *et al.*, Phys. Rev. C **26**, 249 (1982).
[12] M. W. McNaughton and E. P. Chamberlin, Phys. Rev. C **24**, 1778 (1981).
[13] M. W. McNaughton, E. P. Chamberlin, J. J. Jarmer, N. S. P. King, H. B. Willard, and E. Winkelman, Phys. Rev. C **25**, 2107 (1982).
[14] M. W. McNaughton, S. Penttilä, K. H. McNaughton, P. J. Riley, D. L. Adama, J. Bystricky, E. Gülmez, and A. G. Ling, Phys. Rev. C **41**, 2809 (1990).
[15] D. Besset, Q. H. Do, B. Favier, L. G. Greeniaus, R. Hess, C. Lechanoine, D. Rapin, D. W. Werren, and Ch. Weddigen, Phys. Rev. D **21**, 580 (1980).
[16] E. Aprile, R. Hausammann, E. Heer, R. Hess, W. R. Leo, C. Lechanoine-Leluc, S. Morenzoni, Y. Onel, D. Rapin, and S. Mango, Phys. Rev. D **27**, 2600 (1983); E. Aprile *et al.*, *ibid.* **34**, 2566 (1986); a complete amplitude analysis for energies between 447 and 579 MeV is given in R. Hausammann, E. Heer, R. Hess, C. Lechanoine-Leluc, W. R. Leo, Y. Onel, and D. Rapin, *ibid.* **40**, 22 (1989); at 579 MeV see also F. Arash, M. J. Moravcsik, and G. Goldstein, *ibid.* **32**, 74 (1985); and for 800 MeV M. J. Moravcsik, F. Arash, and G. Goldstein, *ibid.*, **31**, 1577 (1985).
[17] T. S. Bhatia *et al.*, Phys. Rev. Lett. **49**, 1135 (1982).
[18] P. Bevington *et al.*, Phys. Rev. Lett. **41**, 384 (1978).
[19] D. A. Bell *et al.*, Phys. Lett. **94B**, 310 (1980).
[20] W. R. Ditzler *et al.*, Phys. Rev. D **29**, 2137 (1984).
[21] I. P. Auer, E. Colton, D. Hill, K. Nield, B. Sandler, H. Spinka, Y. Watanabe, and A. Yokosawa, Phys. Lett. **67B**, 113 (1977); I. P. Auer, E. Colton, H. Halpern, D. Hill, H. Spinka, G. Theodosiou, D. Underwood, Y. Watanabe, and A. Yokosawa, Phys. Rev. Lett. **41**, 354 (1978).
[22] Ed. K. Biegert *et al.*, Phys. Lett. **73B**, 235 (1978); W. de Boer, R. C. Fernow, A. D. Krisch, H. E. Miettinen, T. A. Mulera, J. B. Roberts, K. M. Terwilliger, L. G. Ratner, and J. R. O'Fallon, Phys. Rev. Lett. **34**, 558 (1975).
[23] N. Hoshizaki, Prog. Theor. Phys. **60**, 1796 (1978), the HOSH PSA.
[24] J. Bystricky, C. Lechanoine-Leluc, and F. Lehar, J. Phys. (Paris) **48**, 199 (1987), the SACL PSA.
[25] R. A. Arndt, L. D. Roper, R. A. Bryan, R. B. Clark, B. J. VerWest, and P. Signell, Phys Rev. D **28**, 97 (1983), the VPI PSA.
[26] D. V. Bugg, Phys. Rev. C **41**, 2708 (1990), the Bugg PSA.
[27] R. Dubois, D. Axen, R. Keeler, M. Comyn, G. A. Ludgate, J. R. Richardson, N. M. Stewart, A. S. Clough, D. V. Bugg, and J. A. Edgington, Nucl. Phys. **A377**, 554 (1982), the BASQUE PSA.
[28] D. B. Barlow *et al.*, Phys. Rev. C **37**, 1977 (1988).
[29] G. R. Goldstein and M. J. Moravcsik, Phys. Rev. D **26**, 3026 (1982).